Extended Data

Additive Manufacturing of Hierarchically Porous Silicon-based Ceramics

Ahmad R. Norouzi[a], Brett Paull[a,], Vipul Gupta[a*]

[a]Australian Centre for Research on Separation Science (ACROSS), School of Natural Sciences, University of Tasmania, Hobart, Tasmania 7001, Australia

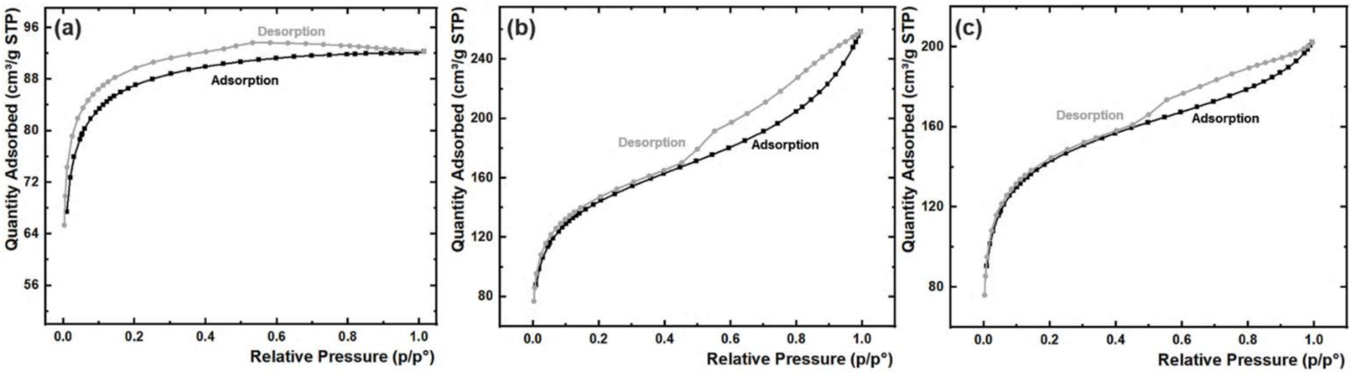

Figure S1. Brunauer–Emmett–Teller (BET) theory-based adsorption isotherms for 3D printed (a) unimodal, (b) bimodal, and (c) trimodal porosity black glass.

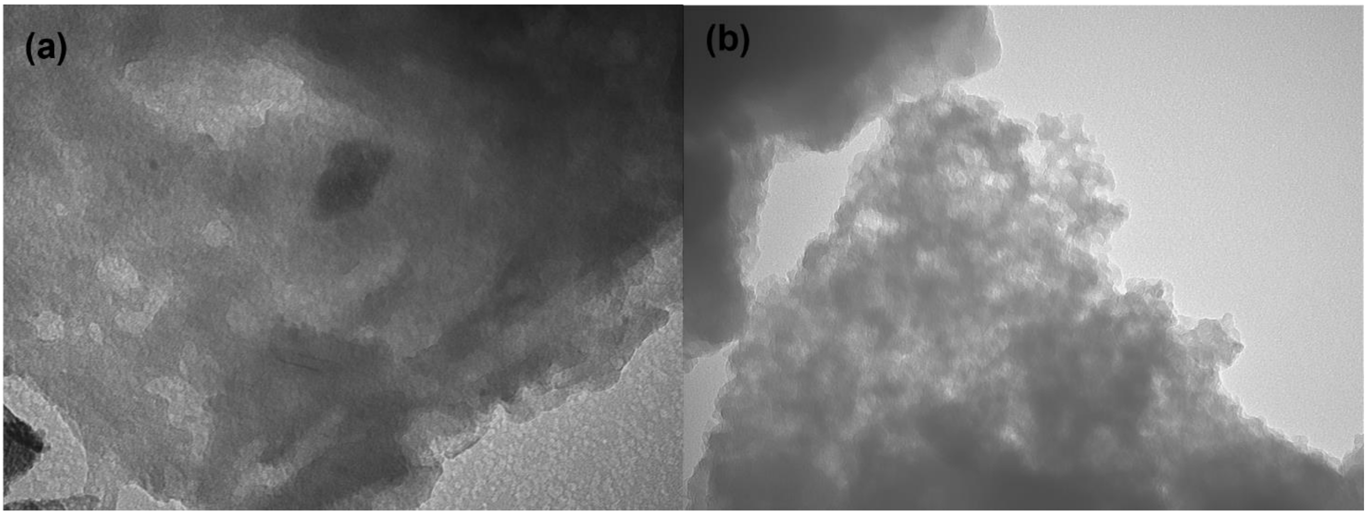

Figure S2. Transmission electron microscope (TEM) images of (a) unimodal and (b) bimodal porosity black glass.

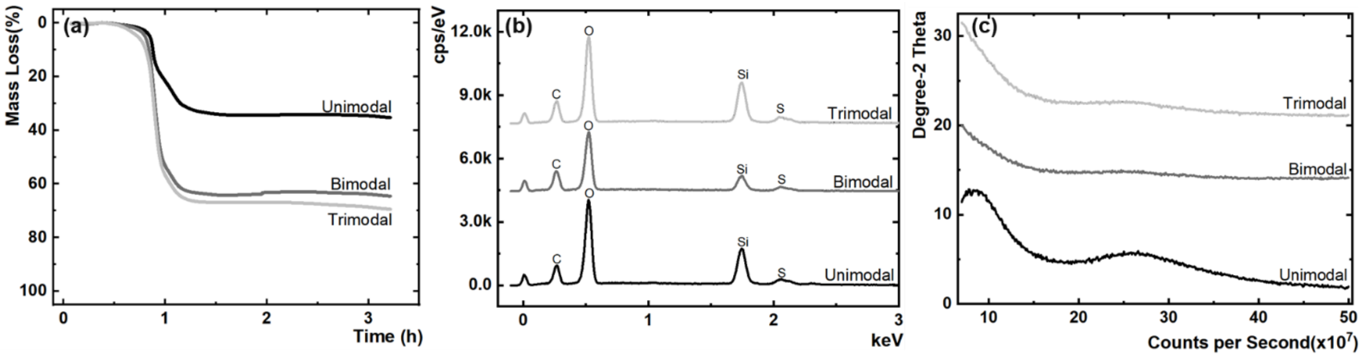

Figure S3. Material characterisation of the 3D printed unimodal, bimodal, and trimodal porosity black glass and the respective resins: (a) thermogravimetric analysis of the unimodal (black), bimodal (dark grey), and trimodal (light grey) porosity resins, (b) elemental analysis of the printed unimodal (bottom), bimodal (middle), and trimodal (top) porosity black glass; and (c) X-ray diffraction analysis of the printed unimodal (bottom), bimodal (middle), and trimodal (top) porosity black glass.

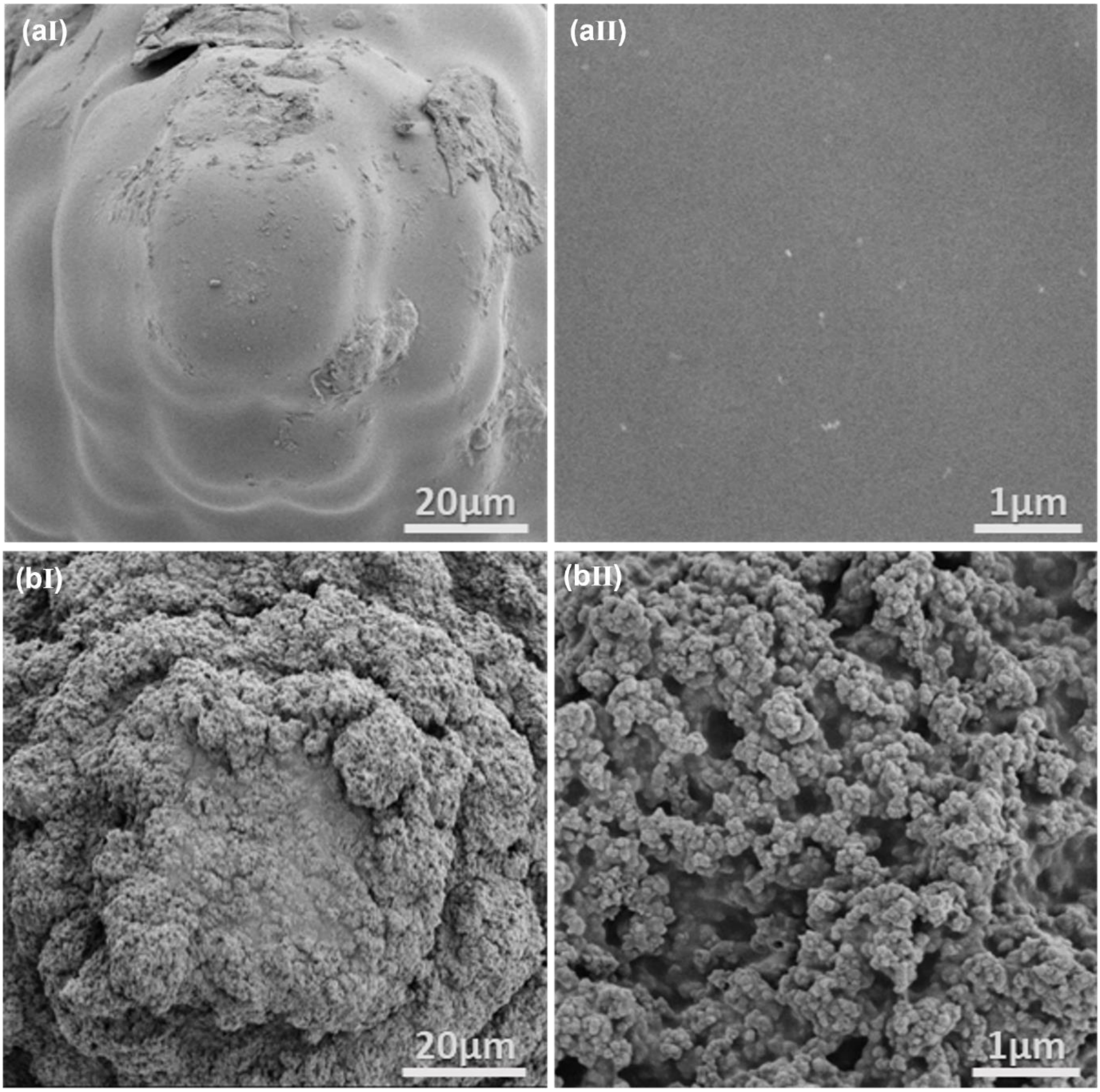

Figure S4. Scanning electron microscope (SEM) images of the microneedles printed with a high and low ceramic yield polymer-based resin system in the (a) absence and (b) presence of mesoporous ceramic nanoparticles.

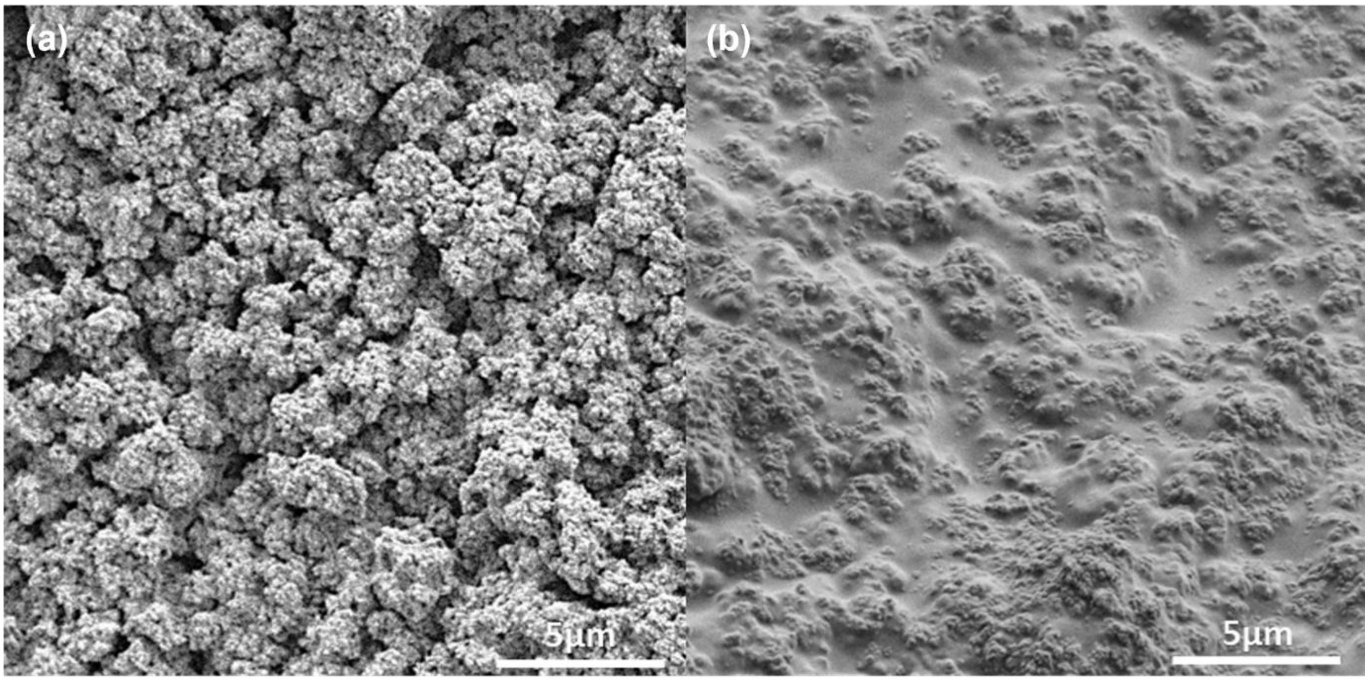

Figure S5. SEM images of the microneedles printed with high and low ceramic yield polymers and mesoporous ceramic particles-based resin system with (a) polyethylene glycol (MW of 400) and (b) polyethylene glycol diacrylate (MW of 575) as the porogens.

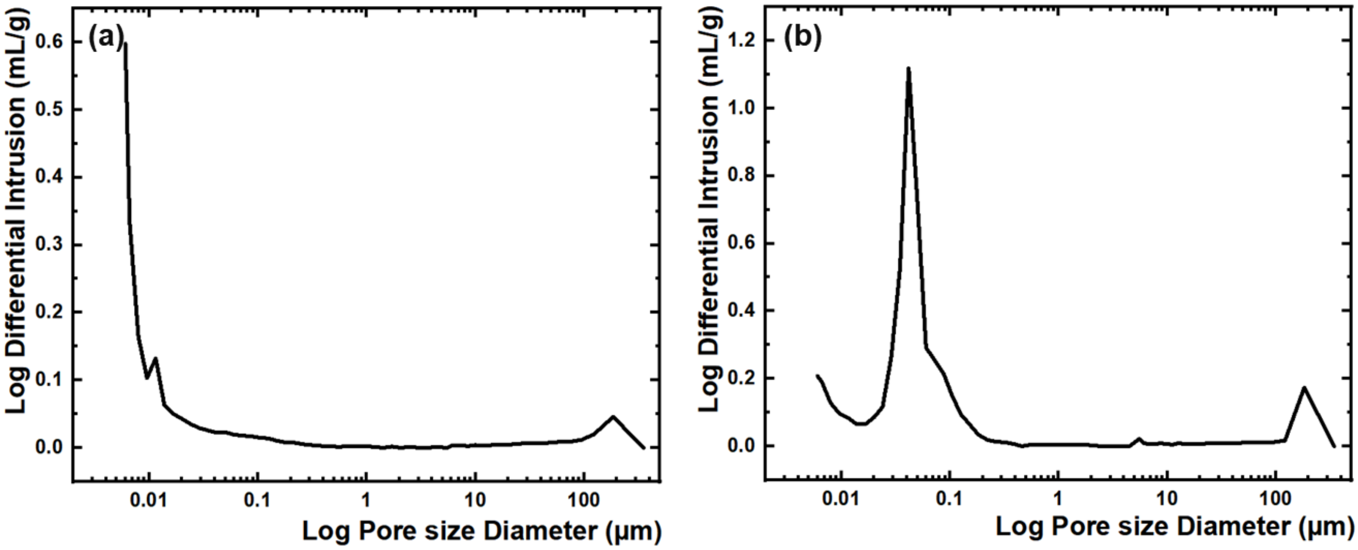

Figure S6. Pore size distribution obtained from mercury porosimetry for (a) bimodal and (b) trimodal porosity black glass.